Materials Chemistry and Physics 302 (2023) 127756

Contents lists available at ScienceDirect

Materials Chemistry and Physics

journal homepage: www.elsevier.com/locate/matchemphys

Full Length Article

Effects of thermomechanical treatments on Cu–Al–Mn Shape Memory Alloys

Dusan Milosavljevic [a,*], Paola Bassani [b], Simone Cinquemani [a], Nora Lecis [a]

[a] Politecnico di Milano, Via Giuseppe La Masa 1, Milan, 20156, Italy
[b] CNR ICMATE, National Research Council, Institute of Condensed Matter Chemistry and Technologies for Energy, Unit of Lecco, Via Previati 1/e, Lecco, 23900, Italy

HIGHLIGHTS

- Hot-rolling achieves low SMA sheet thickness, but introduces a possibility of oxidation, thus a change of material properties.
- Temperature cycling stabilizes transformation temperatures, but above a certain range leads to martensitic stabilization.
- Application of static preload on Cu–Al–Mn alloys show potential for improved damping performance.
- Increased frequency range of damping estimation expands available information about the Cu–Al–Mn alloy damping performance.

ABSTRACT

In this paper, the authors, building on the established state-of-the-art knowledge, explore the effects of thermomechanical treatments on the Shape Memory Effect (SME) and damping performance of the Cu–Al–Mn Shape Memory Alloys (SMA). Specifically, to explore the potential of application of this SMA in the form of sheets, for the purpose of designing lightweight structures with high damping performance. The casting and the thermomechanical treatment process were fully laid out in the paper. The characterization of the material in terms of chemical composition and microstructure was performed through optical microscopy and SEM coupled with EDX analysis. The temperature-induced phase transformation behavior of the alloy was explored using DSC. The damping performance was quantified through the loss factor which was measured at different levels of static tensile preload using a DMA machine. The alloy has shown significant workability which permits the fabrication of sheets. However, the material displays high sensitivity to oxidation due to a combined effect of impurities and the hot-rolling process necessary for obtaining thin SMA sheets. Nonetheless, the alloy shows competitive damping performance with respect to commercially available NiTi SMA.

1. Introduction

Interest in shape memory alloys (SMAs) as a material for vibration damping application stems from the fact that beyond the intrinsic damping which is inherent to all materials, two additional phenomena can be observed in SMA behavior. First, while in a twinned martensitic state, the alloys exhibit a damping potential as a consequence of internal friction which occurs when the material is under load and experiences de-twinning of the martensitic structure [1]. Second, a sharp increase in the value of damping occurs during both reverse martensitic transformation (heating) [2], and direct martensitic transformation (cooling) [3]. However, the increase in damping during transformation is not intrinsic, it is a function of the heating and cooling rates [1,2]. Furthermore, the value of material damping is higher in the martensitic phase than in the parent phase [3]. The first mechanism of damping, given its dependence on external loading factors, could potentially be applied in semi-passive damping components. Conversely, the damping increase given by martensitic transformation opens up a possibility of active damping control. NiTi SMAs represent the most widely researched and used alloys within the industry as sensors, actuators, and in other applications. The search for a substitute alloy is primarily motivated by the goal of reducing costs. Cu-based alloys have received significant attention because copper is cheaper than Ni and Ti. Furthermore, Cu-based alloys offer ease of fabrication, as well as competitive strain recovery and damping properties with respect to NiTi SMAs. However, these advantages are offset by their intrinsic brittleness, aging-based martensite stabilization, and other issues [4]. Over the course of nearly three decades, periodic efforts have been made to improve the properties of Cu–Al–Mn SMAs by expanding the knowledge related to their composition, fabrication, and thermomechanical treatment. Controlling the content and ratio of aluminum and manganese within the alloy has proven to have significant effects on transformation temperatures, material workability, and the typology of the martensitic structure that can be obtained [5–8]. As presented by Kainuma et al. In

* Corresponding author.
E-mail address: dusan.milosavljevic@polimi.it (D. Milosavljevic).

https://doi.org/10.1016/j.matchemphys.2023.127756
Received 4 November 2022; Received in revised form 16 February 2023; Accepted 9 April 2023
Available online 10 April 2023

Ref. [7], slight changes in chemical composition, in the order of a percentage point fraction, have the possibility of shifting phase transformation temperatures of the alloy by tens of degrees Celsius [5]. Depending on the aluminum content in Cu–Al–Mn alloys, the material will present with different forms of martensite; low Al content, under 18% at., results in 2 M martensite phase formation upon quenching from the stable β-phase region; while higher content results in 6 M martensite. Lower Al content in the alloy produces a structure with a higher degree of disorder, resulting in higher material workability [5]. Adjustments to workability, damping, and pseudoelasticity properties can be made by controlling the relative grain size in the alloy, as well as the material texture [2,3,5,9–11]. Specifically, an increase in relative grain size causes a significant improvement in recoverable strain, reaching values of 7% at a relative grain size of d/t ≈ 15, where d and t are defined as mean grain size and sheet thickness, respectively [11]; while the loss factor when the alloy is in martensitic phase reaches values of tanδ ≈ 0.04 [2] The effect of aging temperature on Cu–Al–Mn alloy microstructure and transformation characteristics has also been explored in Ref. [12]. Likewise, adjustments to transformation temperatures, workability, and shape memory properties can be achieved by including additional alloying elements [13]. The extensive research outlined above has led to several potential applications of Cu–Al–Mn with both small and large dimensions of devices being considered. Cu–Al–Mn alloys have already shown superior performance to NiTi wires in medical application as guidewires for catheterisation, but also with a possiblity that these SMA microtubes will find other applications as well [9,14]. Furthermore, the high damping potential resulting from grain size and texture control makes them attractive for seismic applications in civil engineering as seismic dampers and isolators for buildings [15,16]. The research effort of the authors of this paper is related to the application of SMAs in laminated form as elements of lightweight composite structures intended for vibration damping application. These kinds of composite materials would require SMA sheets whose thickness is in the order of a fraction of a millimeter. This requirement is a practical one, in composite materials, as it allows for effective layer embedding and higher delamination resistance of the final composite structure. As such, Cu-based SMAs and Cu–Al–Mn alloys specifically, were a material of interest, given the ratio between their price and their damping performance, as well as the potential for improved workability. Relying on the established knowledge of Cu–Al–Mn alloys, the authors attempted in the present paper to choose the appropriate composition, fabricate, shape, and treat the Cu–Al–Mn alloy, to prepare it for application. This process, the related results, and the issues faced, will be laid out in this paper and discussed.

2. Experimental process

2.1. Alloy preparation

The selected composition for the alloy was Cu–16Al–10Mn % at., corresponding to Cu-7.6Al–Mn9.67 % wt. The alloy was prepared by starting from pure Cu, Al, and Mn, whose chemical purity and form are described in Table 1. The presence of a low amount of phosphorus in the copper pellets comes as a consequence of the copper production process where phosphorus is used to avoid the oxidation of copper.

The casting process of the chosen Cu–Al–Mn alloy was performed in the facilities of CNR-ICMATE in Lecco, Italy, using an Induction Melting Furnace (Ages-Galloni), equipped with a graphite crucible, and operated with a mild stream of Ar acting as a protective atmosphere. As manganese is highly reactive to oxygen, pre-alloys of Cu–Mn were prepared in a vacuum arc melting furnace. The proper amount of copper and aluminum was added to achieve the final composition. The materials were heated until complete melting occurred. After waiting for several minutes for melt homogenization thanks to magnetic stirring, the alloy was cast in a 300 °C preheated graphite mold of 12 × 70 × 120 mm^3. After 5 min from the completion of the casting, the ingot was removed from the mold and quenched in room-temperature water.

Table 1
Raw materials used in the casting process; their purity and form.

Element	Purity [%]	Form
Cu	99.98 (P ~0.04 ÷ 0.06)	Pellet, about 10 g each
Al	99.99	Granules <12 mm
Mn	99.99	Chips fromthe electrolytic process

2.2. Thermomechanical processing

As the intention was to explore the possibility of using this SMA in the form of a thin layer embedded within a composite, the obtained ingot was subjected to thermomechanical processing to produce SMA sheets with a thickness lower than 1 mm. To analyze the effect of rolling and heat treatments, different processing routes were tested, and heat treatments at different thicknesses were performed.

In Fig. 1, a section of the Cu–Al–Mn diagram at 10% at. of Mn is shown, with the red line signifying the target composition of the alloy. A temperature of 900 °C was selected for the homogenization and betatization treatments, as it was deemed sufficiently above the lower boundary of the single β-phase region to guarantee a complete transformation. For two-phase heat treatments, a temperature of 600 °C was chosen because it ensures that, at the selected composition, the alloy will be in the α + β phase region.

Rolling processing was performed in part in the facilities of CNR–ICMATE, and in part at Politecnico di Milano. The first deformation process, at CNR-ICMATE, was performed by hot rolling down to about 2 mm. Subsequently, hot rolling was performed down to the desired final thickness of 0.6 mm, at Politecnico di Milano. In between the rolling steps, observations were made using optical microscopy to determine any presence of cracking. Furthermore, the final samples used in performance characterization were cut from the interior part of the rolled pieces rather than the edges to be more representative.

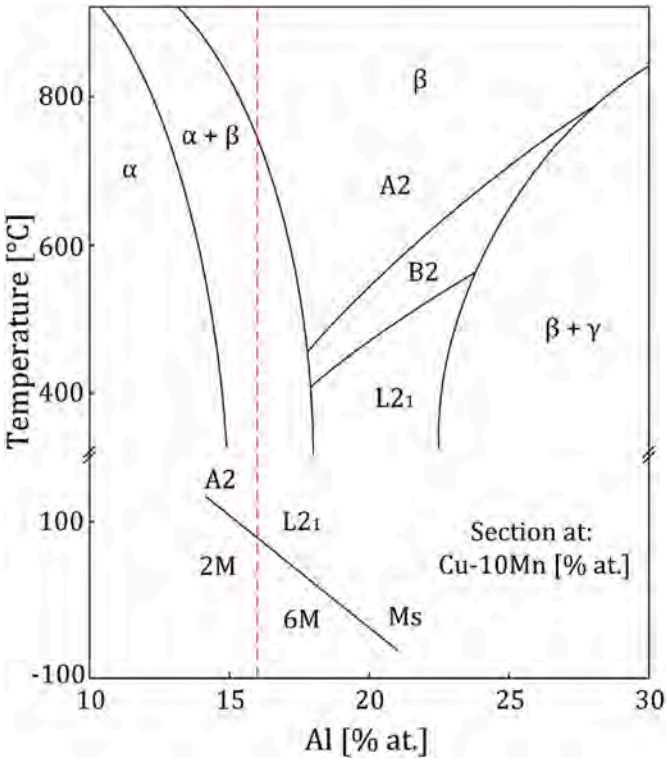

Fig. 1. Isothermal and iso-Mn section of the ternary Cu–Al–Mn phase diagram at 10% at. of Mn, as discussed in Sutou et al. in Ref. [5].

Initial rolling of the alloy was performed in the facilities of CNR–ICMATE using a rolling mill with a roll diameter of 30 cm. The ingot was cut into two pieces of 12 × 35 × 120 mm^3 Each half was preheated at 900 °C for 10 min and then was rolled, with 0.5 mm thickness reduction per iteration. After each pass, the ingot was reheated for about 2 min and 30 s. This was repeated until the final thickness was 2.3 mm, with a reduction of 80%.

To obtain the final thickness, the hot-rolling process was continued in the laboratories at Politecnico di Milano, using a rolling mill with a roll diameter of 15 cm. The process temperature was kept at 900 °C. To avoid any risk of cracks at lower thicknesses, the step after each rolling was reduced from 0.5 mm to 0.3 mm per iteration. In this way, it was possible to reduce the thickness of the SMA samples to about 0.7 mm. Due to the limitations of the machine, at this point, it was necessary to overlap two samples and roll them together to achieve further reduction. The final thickness at the end of the rolling process was 0.6 mm.

2.3. Characterization

Microstructural characterization was performed using an optical (OM, Nikon ECLIPSE LV150NL) and a scanning electron microscope (SEM, Zeiss Sigma 500), the latter coupled with an Energy-Dispersive X-ray (EDX, Oxford Instruments Ultim Max 65) detector, that was employed to track the composition of the SMA.

Transformation temperatures were monitored with Differential Scanning Calorimetry (DSC, Q25, TA Instruments) analysis. Analyses were performed on samples with weight ranging in the interval 20 ÷ 100 mg, with cooling heating rates of 10 °C/min, in the −50 ÷ 200 °C temperature range. At least two heating/cooling steps were performed on each specimen. Selected specimens were also manually thermal-cycled between liquid nitrogen and hot boiling water and then tested again.

Dynamic mechanical analysis (DMA) was performed to quantify the damping potential of the Cu–Al–Mn alloy. The tests were conducted using the Anton Paar MCR 702 MultiDrive. Information on material damping is obtained through the loss factor tanδ, which was calculated as:

$$tan\ \delta = \frac{E''}{E'} \quad (1)$$

here E' [MPa] and E'' [MPa] are the storage and loss moduli, as measured by the machine, respectively.

All tests were carried out in tensile mode. The samples were prepared by taking the hot rolled, betatized, and quenched Cu–Al–Mn, and using a micro-cutting machine to cut each sample. The cross-section of the samples had an average area of 0.3 mm^2, the thickness after rolling was consistently between 0.55 and 0.6 mm, while there were slightly larger variations in width due to the precision of the micro-cutter.

The length of the samples was 65 mm. This choice of dimensions was based on the 40 N load capacity of the DMA machine, hence it was necessary to reduce the cross-section to apply meaningful stress as well as maintain the compliance necessary for accurate measurements. The first part of the testing process involved a strain sweep in the range of [0.0001, 0.1] % of strain amplitude, at 1 Hz frequency and 10 N of static preload. The second block of tests was based on frequency sweeps. The range of tested frequencies was [0.1, 100] Hz, with ten measurement points per decade. These frequency sweeps were done across a range of static preloads [5,10] N in increments of 5 N.

3. Results and discussion

The primary concern while choosing the exact composition of the alloy was to obtain an SMA with a satisfactory degree of shape memory properties in combination with ductility that would allow for the shaping of the material. The choice of Cu–16Al–10Mn % at. was made. Looking at the work done by Sutou et al. In Ref. [5], this composition was expected to result in shape recovery near 90% and cold workability of nearly 80%, with cold workability defined as $W = (t_0\text{-}t_{min})/t_0 \cdot 100$, such that t_0 and t_{min} are the initial and minimum thickness before cracking while cold-rolling at room temperature, respectively. The second consideration made while choosing the composition was related to the phase transformation temperatures. As mentioned in the introduction, the spike in damping that occurs during both martensitic and reverse martensitic transformations introduces a potential for active damping control during application. However, for application, it was necessary to ensure that transformation temperatures are within a range that can be achieved in practice. For this reason, the aim was to have an alloy with transformation temperatures close to 100 °C. This would make the potential transformation achievable while ensuring it is not accidently triggered by being too close to the room temperature. Cu–Al–Mn alloys show a wide range of possible phase transformation temperatures which are highly sensitive to relatively small alterations in the composition, as shown in the work of Mallik et al. [6]. The results provided by Kainuma et al. [7] show that for Cu–16Al–10Mn % at. the expected transformation temperatures are $M_s = 80$ °C, $M_f = 60$ °C, $A_s = 84$ °C, $A_f = 97$ °C.

During the rolling process described in Section 2.2. between the rolling stages, multiple observations via optical microscopy did not reveal any significant cracks while attempting to reach the desired thickness of 0.6 mm. A section of the material as hot rolled is shown in Fig. 2: even if preheating at 900 °C was performed, a two-phase structure

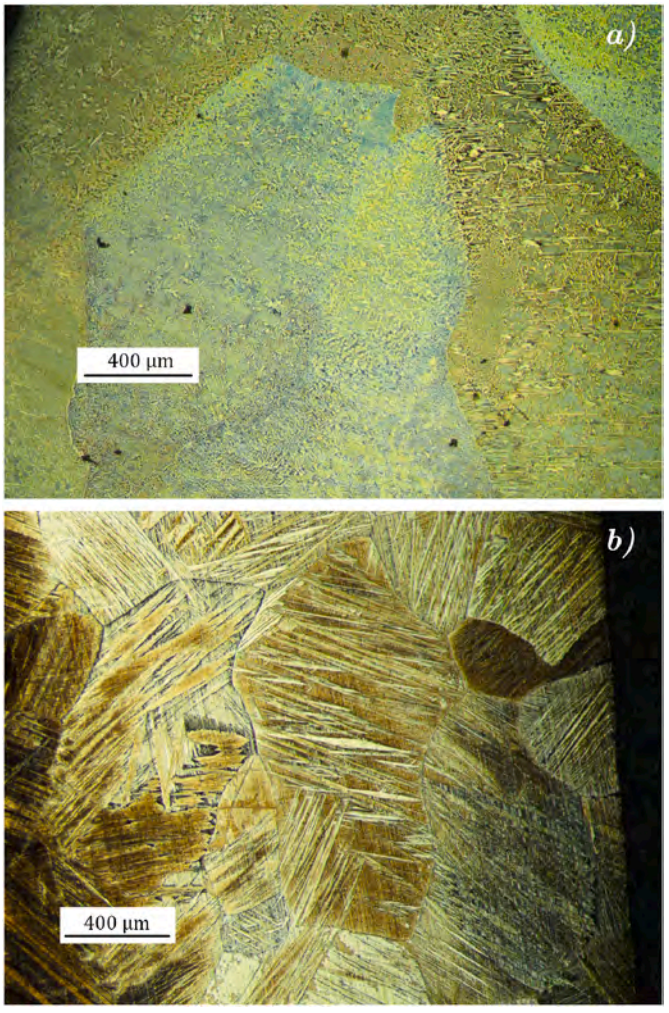

Fig. 2. Cu–Al–Mn alloy microstructure after initial hot rolling to a thickness of 2.3 mm: a) before betatization, b) after betatization.

was observed, that disappeared after betatization and quenching. No trace of the initial solidification structure could be observed, but an extensive grain coarsening can be appreciated, with a mean grain size of d = 632 μm.

The betatization and quenching is a critical thermal treatment that allows us to bring out the shape memory behavior in the alloy. It involves heating the SMA samples to a temperature sufficient to obtain a stable β-phase, then quenching them to obtain a martensitic structure. The laminated samples were heated in the furnace at 900 °C for 30 min and afterward quenched in water at around 10 °C.

In Figs. 2 and 3, it is possible to observe the effects of the betatization process on the Cu–Al–Mn initially hot rolled to 2.3 mm and hot rolled to 0.6 mm, respectively. In both cases, the effect of the heating of the samples to the region of stable β-phase and subsequent quenching resulted in obtaining a familiar morphology characteristic of martensitic structures. Moreover, a set of samples hot rolled to a thickness of 0.6 mm were betatized for differing amounts of time (15, 30, and 45 min) and afterward observed under an optical microscope. No significant change in structure or grain size was observed, with grains showing sizes between 300 and 340 μm across all samples. EDX analysis of the SMA samples revealed that the effect of hot-rolling on the overall composition of the samples was a reduction in manganese content. This effect is shown in Fig. 4. After further thickness reduction through hot rolling, a drop of around 2% at. in manganese was observed. There was no significant change in aluminum content, and the values shown in Fig. 4 correspond to a readjustment in the composition ratio as a consequence

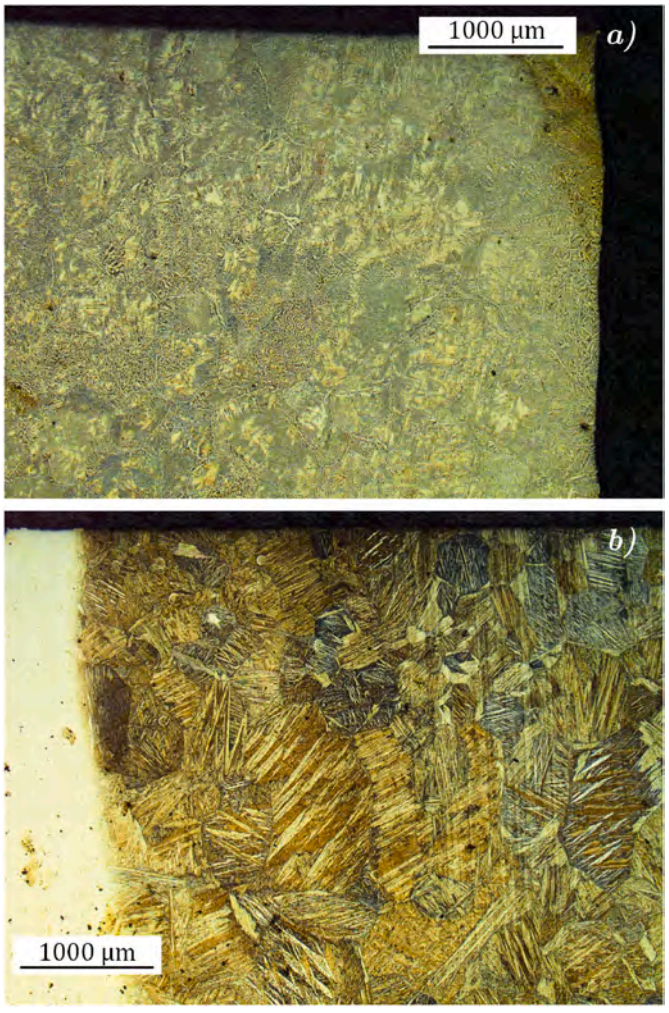

Fig. 3. Cu–Al–Mn alloy microstructure after hot rolling to a thickness of 0.6 mm: a) before betatization, b) after betatization.

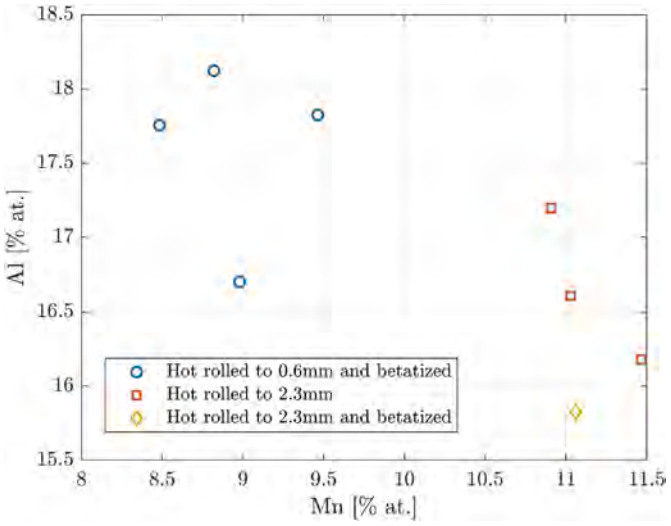

Fig. 4. Decrease in Mn content as a consequence of thermomechanical treatment measured by EDX.

of manganese loss. Additionally, EDX analysis revealed the presence of trace amounts of phosphorus, ranging between 0.1 and 0.2% at. depending on the sample. The presence of phosphorus inside the alloy resulted in the formation of manganese-phosphide precipitates which can be observed in Fig. 5a, as green spots. Moreover, during the rolling process, a significant level of oxidation was observed, in particular that of the phosphorus precipitates, shown in Fig. 5b, orange spots. This effect was further highlighted with the oxidized precipitates showing brighter red in Fig. 6b. The composition of the precipitates given in Table 2 shows that manganese is bound inside the precipitates instead of being distributed throughout the alloy. Additionally, the main effect of oxidation is the loss of manganese.

DSC analysis of SMA samples that were hot rolled to 2.3 mm thickness, betatized, and quenched, revealed that thermal cycling caused stabilization of phase transformation temperatures. The exact values of the phase transformation temperatures during cycling are given in Table 3, while the first and final cycles of the DSC analysis are shown in Fig. 8. The discrepancy between the obtained final phase transformation temperatures and those that were expected based on the aimed composition of the alloy was attributed to the effect of precipitation. Namely, the reduced amount of manganese present in the solid solution of the alloy means that the final obtained composition is a couple of percentage points away from the aimed values of manganese content. However, DSC testing carried out on Cu–Al–Mn samples that were hot rolled to a thickness of 0.6 mm and betatized revealed that no phase transformation occurs and that martensite becomes fully stable. Furthermore, cycling of the previous 2.3 mm thick samples at temperatures above 300 °C was observed to result in complete martensitic stabilization and no further phase transformation, see Fig. 7.

The results obtained in the strain sweep testing of the Cu–Al–Mn samples revealed a strong dependency of the loss factor tanδ on the strain amplitude during testing. In Fig. 9, it can be observed that initially, for strain amplitude values below 0.006%, the behavior of the material is seemingly random. This phenomenon was attributed to the use of strain amplitude values which are very close to the precision level of the DMA machine itself. As such, they were disregarded from further consideration. Moreover, starting at 0.01% and with a further increase in strain amplitude, the loss factor tanδ exhibits a linearly increasing behavior. This was measured up to a strain amplitude of 0.097% where a tanδ value of 0.948 was recorded. This alloy behavior is consistent with the load-dependent mechanism of damping observed in SMAs which is related to the increase of internal friction as a consequence of detwinning under load [1]. Examples of this loss factor dependency, attributed

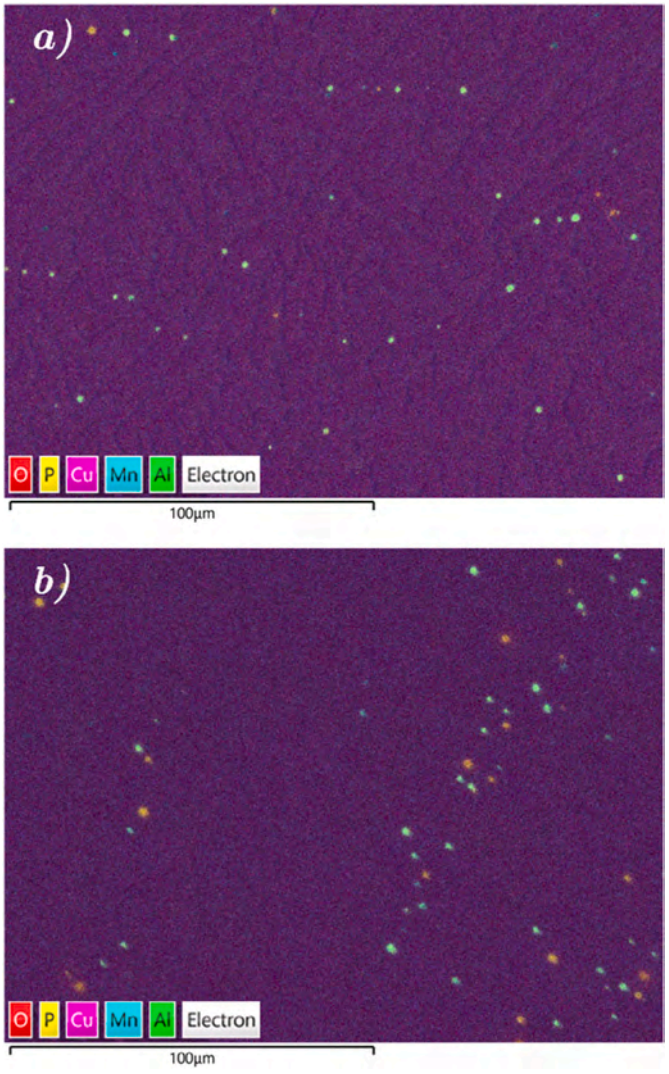

Fig. 5. SEM map highlighting the phosphorus precipitates inside the SMA and their oxidation: a) Cu–Al–Mn hot rolled to 2.3 mm with precipitates containing high amount of Al Mn prior to oxidation, b) Cu–Al–Mn hot rolled to 0.6 mm with precipitates showing high oxidation through a change in color from green to orange. (For interpretation of the references to color in this figure legend, the reader is referred to the Web version of this article.)

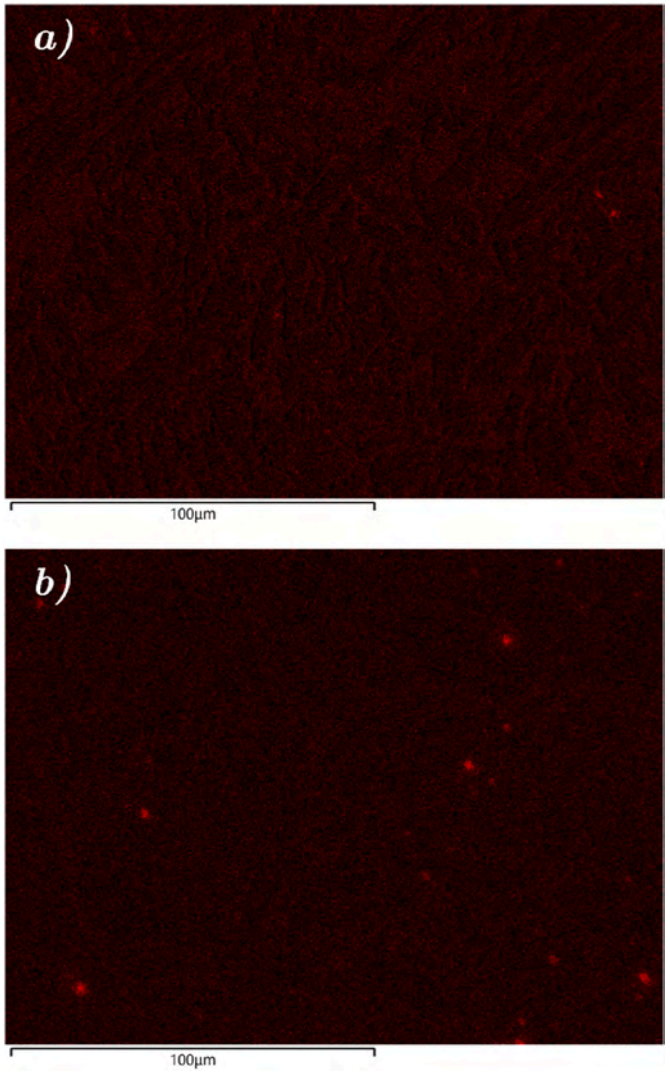

Fig. 6. SEM map highlighting the oxidation of Mn in phosphorus precipitates inside the SMA due hot rolling: a) Cu–Al–Mn hot rolled to 2.3 mm, b) Cu–Al–Mn hot rolled to 0.6 mm.

to the mechanism of hysteretic movement of martensitic variant interfaces, on strain amplitude in NiTi and Ti–Nb SMAs can be found in Refs. [17,18], respectively. To reduce the effect of strain amplitude on any further measurements made on the DMA machine, a strain amplitude of 0.01% was selected for all subsequent testing.

As previously stated, the second block of tests was based on a series of frequency sweeps at varying levels of static preload. In Table 4, the exact values of imposed static preload and the resulting measured values of static prestress are shown. Additionally, a stress amplitude which was measured as a consequence of the imposed strain amplitude of 0.01% was also given.

The measured tanδ values during the strain sweep testing are shown in Fig. 10 for each value of static preload.

Firstly, a highly non-linear behavior of tanδ is observed for frequencies below 1 and above 20 Hz, for all measurements regardless of static preload. Since this behavior was also observed during testing of other materials, such as brass, that do not possess characteristics inherent in shape memory alloys, this behavior was verified as being an artifact of the DMA machine, and hence it was disregarded. For further considerations, a focus was placed on the tanδ values obtained in the

Table 2
Composition corresponding to phosphorus precipitates before and after oxidation, respectively.

Precipitate [#]	Composition [% at.]				
	Cu	Al	Mn	P	O
1	15.4	4	50	27.4	3.2
2	32.5	5.4	9.1	29.4	23.7

Table 3
Transformation temperatures that were obtained through repeated thermal cycling of the alloy in the range of −100 to 150 °C.

Cycle [#]	A_s [°C]	A_f [°C]	M_s [°C]	M_f [°C]
1	−41	−5	−23	−58
2	10	49	32	−6
3	21	60	44	5
4	28	64	46	9
5	32	70	49	13
6	35	73	52	17

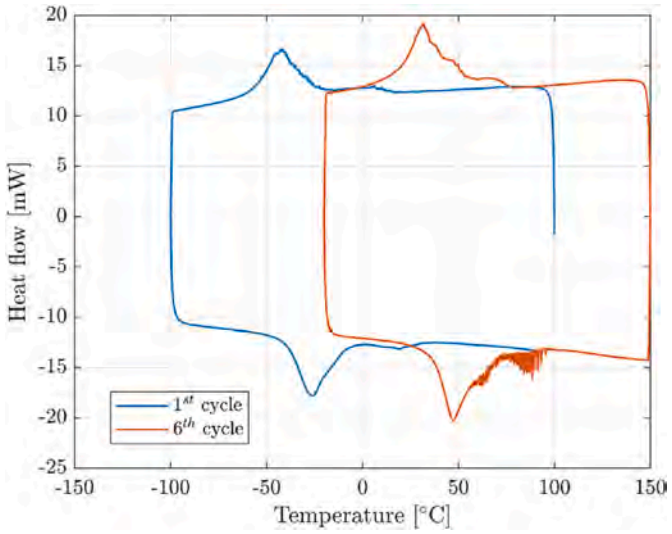

Fig. 7. Stabilization and loss of phase transformation due to heating above 300 °C.

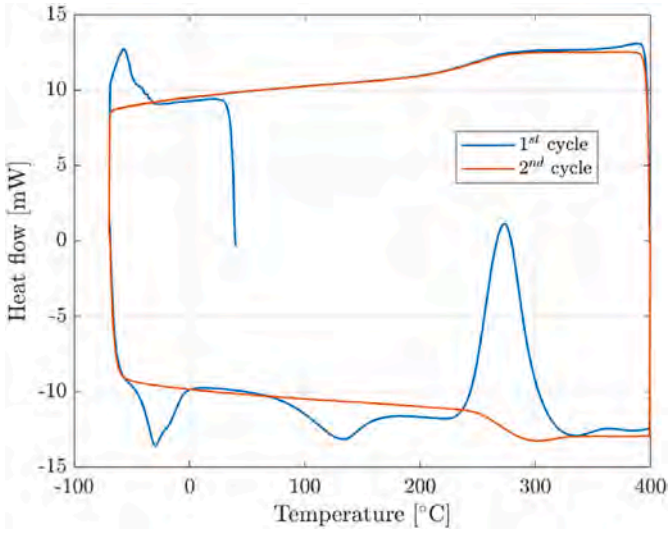

Fig. 8. Transformation peaks of Cu–Al–Mn during the 1st and 6th (final) thermal cycle.

range [1, 20] Hz. A phenomenon that can be seen is that starting from the low level of static preload at 5 N, an incremental increase of tanδ is observed across the frequency range with each increase in preload up to 20 N, after which there is an incremental decrease. To better observe this phenomenon, data were rearranged in Fig. 11a and b. The values of tanδ were averaged across the frequency range [0, 20] Hz for each static preload level, and tanδ vs preload for individual frequencies and shown in Fig. 11a and 11b, respectively. A dependency of mean tanδ on static preload can be observed. The mean values of the loss factor measured, range from 0.014 to 0.02.

In the interest of comparing the measured performance of the fabricated Cu–Al–Mn alloy with respect to that of other materials, testing under equivalent conditions was performed for commercially available thin sheet samples made of brass and samples made of NiTi. The measured damping performance of these materials is shown in Fig. 12. Frequency sweeps performed on NiTi show a similar effect of static preload as the one observed in Cu–Al–Mn, while the same effect is negligible in brass.

A further comparison of damping performance between these

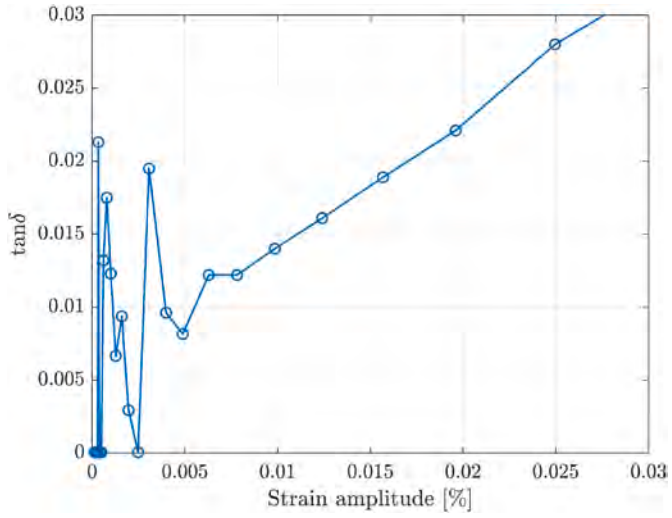

Fig. 9. Damping behavior measured during a strain sweep performed at 1 Hz oscillation frequency and 10 N of static preload.

Table 4
Values of imposed static preload and the measured values of static prestress and stress amplitude during DMA.

Static preload [N]	Static prestress [MPa]	Stress amp. [MPa]
5	14	75
10	38	75
15	62	75
20	86	75
25	110	75
30	134	75
35	158	75

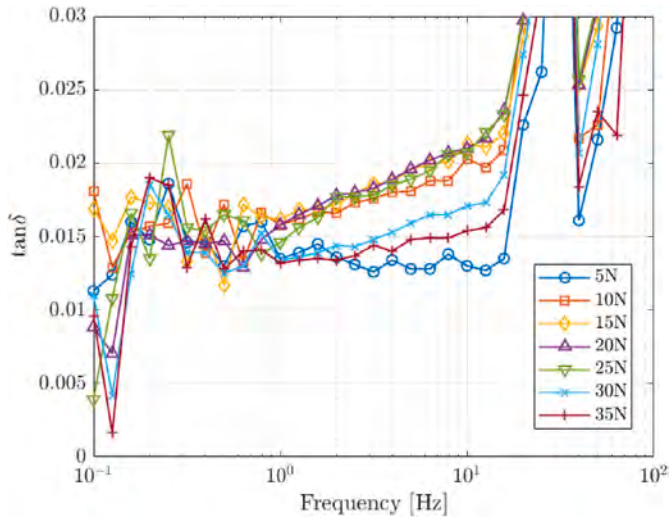

Fig. 10. Damping behavior of Cu–Al–Mn measured during frequency sweeps for a range of static preloads [5, 35] N with a step of 5 N per iteration.

materials is given in Fig. 13. Firstly, across all values of static preload, the Cu–Al–Mn alloy shows a higher damping performance than NiTiNOL, as well as that of brass. Furthermore, it is possible to observe a higher level of sensitivity of the loss factor to static preload in Cu–Al–Mn, with respect to the other tested materials.

One of the possible explanations as to the cause of an increase in damping under preload is related to the initiation of the de-twinning of martensite, a phenomenon that improves damping due to increased

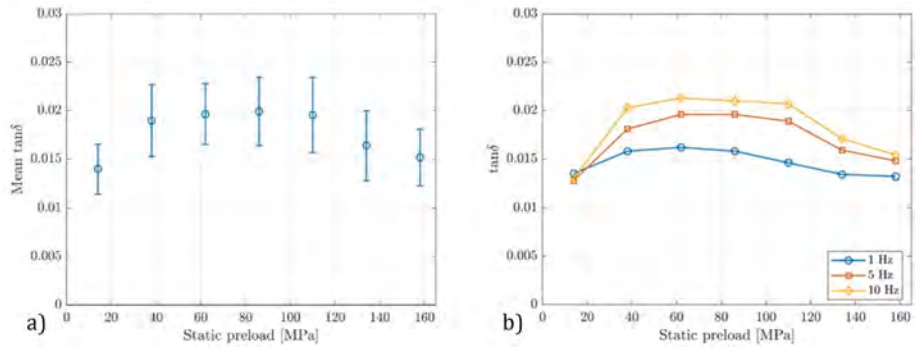

Fig. 11. a) Values of tanδ averaged across the range of frequencies [1, 20] Hz for each value of the applied static preload, and their corresponding standard deviations. b) Values of tanδ measured at 1 Hz, 5 Hz, and 10 Hz for each value of the applied static preload.

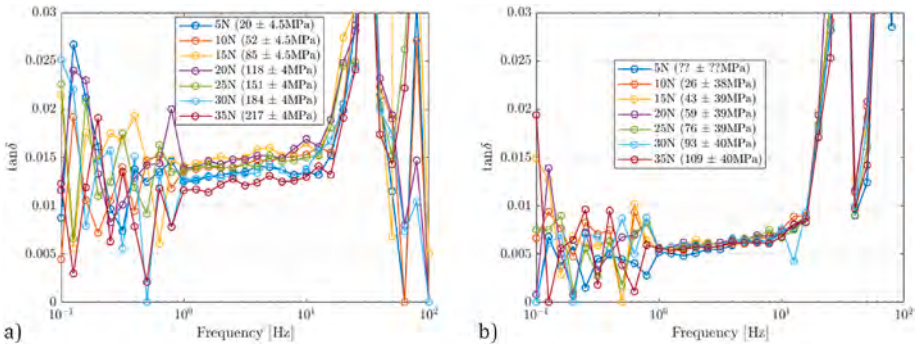

Fig. 12. Damping behavior measured during frequency sweeps for a range of static preloads [5, 35] N with a step of 5 N per iteration, on: a) NiTi, b) brass.

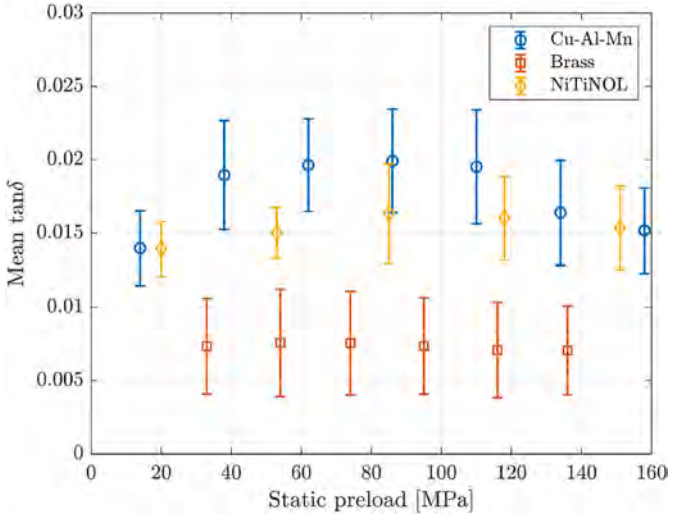

Fig. 13. The values of tanδ measured for this Cu–Al–Mn alloy compared to the values measured in brass and NiTiNOL tested under the same parameters.

internal friction during de-twinning. The difficulty in confirming this is that the effect of this increase is related to a dynamic phenomenon, making it hard to observe independently.

4. Conclusions

1. The choice of the Cu–16Al–10Mn % at. has shown to provide the workability of the material necessary for the shaping process of lamination.
2. Due to the high reactivity of manganese, exceptional care must be taken during acquisition of pure materials. In particular, copper, as it often comes with trace amounts of phosphorus present. Moreover, adjustments in the casting process should be made to account for the possible presence of phosphorus, and likely loss of manganese.
3. While the obtained transformation temperatures are close to the desired range of about 100 °C, further study of the phase stabilization phenomenon is necessary. Especially, as there is a strong possibility of its relation to the oxidation that occurs as the samples are laminated to ever-lower thicknesses by hot rolling.
4. It is necessary to conduct further inquiry into the effect of manganese-phosphides on the behavior of the alloy.
5. The obtained damping performance in martensitic form of the Cu–16Al–10Mn % at. alloy after treatment was shown to be competitive with that of commercial NiTi SMA.
6. The SMA alloy behavior suggests a potential for the use of static preload during alloy application for the purpose of damping performance tunability.

CRediT authorship contribution statement

Dusan Milosavljevic: Methodology, Validation, Investigation, Writing – original draft, Writing – review & editing, Visualization. **Paola Bassani:** Investigation, Writing – review & editing. **Simone Cinquemani:** Supervision, Project administration, Funding acquisition. **Nora Lecis:** Supervision, Project administration, Writing – review & editing.

Declaration of competing interest

The authors declare that they have no known competing financial interests or personal relationships that could have appeared to influence the work reported in this paper.

Data availability

Data will be made available on request.

Acknowledgment

This work was supported by the Office of Naval Research under grant N00014-20-1-2608.

The authors would like to acknowledge Mr. N. Bennato and E. Bassani for their technical assistance during alloy melting and rolling at CNR – ICMATE.

References

[1] J. San Juan, M.L. Nó, Damping behavior during martensitic transformation in shape memory alloys, J. Alloys Compd. 355 (1-2) (Jun. 2003) 65–71, https://doi.org/10.1016/S0925-8388(03)00277-9.

[2] Y. Sutou, T. Omori, N. Koeda, R. Kainuma, K. Ishida, Effects of grain size and texture on damping properties of Cu-Al-Mn-based shape memory alloys, Mater. Sci. Eng., A 438–440 (SPEC. ISS) (Nov. 2006) 743–746, https://doi.org/10.1016/j.msea.2006.02.085.

[3] N. Koeda et al., "Damping Properties of Ductile Cu-Al-Mn-Based Shape Memory Alloys * 1.".

[4] K.K. Alaneme, E.A. Okotete, Reconciling viability and cost-effective shape memory alloy options – a review of copper and iron based shape memory metallic systems, Eng. Sci. Technol. Int. J. 19 (3) (Sep. 2016) 1582–1592, https://doi.org/10.1016/j.jestch.2016.05.010.

[5] Y. Sutou, T. Omori, R. Kainuma, K. Ishida, Ductile Cu-Al-Mn based shape memory alloys: general properties and applications, Mater. Sci. Technol. 24 (8) (2008) 896–901, https://doi.org/10.1179/174328408X302567.

[6] U.S. Mallik, V. Sampath, Effect of composition and ageing on damping characteristics of Cu-Al-Mn shape memory alloys, Mater. Sci. Eng., A 478 (1–2) (Apr. 2008) 48–55, https://doi.org/10.1016/j.msea.2007.05.073.

[7] R. Kainuma, S. Takahashi, K. Ishida, Ductile shape memory alloys of the Cu-Al-Mn system, J. Phys. IV 5 (C8) (1995). C8-961.

[8] R. Kainuma, S. Takahashi, K. Ishida, Thermoelastic martensite and shape memory effect in ductile Cu-Al-Mn alloys, Metall. Mater. Trans. A 27 (8) (1996) 2187–2195.

[9] Y. Sutou, T. Omori, J. Wang, R. Kainuma, K. Ishida, Characteristics of Cu–Al–Mn-based shape memory alloys and their applications, Mater. Sci. Eng., A 378 (1–2) (2004) 278–282.

[10] Y. Sutou, T. Omori, K. Yamauchi, N. Ono, R. Kainuma, K. Ishida, Effect of grain size and texture on pseudoelasticity in Cu–Al–Mn-based shape memory wire, Acta Mater. 53 (15) (2005) 4121–4133.

[11] Y. Sutou, T. Omori, R. Kainuma, K. Ishida, Grain size dependence of pseudoelasticity in polycrystalline Cu–Al–Mn-based shape memory sheets, Acta Mater. 61 (10) (2013) 3842–3850.

[12] K. Yildiz, Effect of aging on structure and shape memory behavior of a Cu-Al-Mn-Ti-C shape memory alloy, Thermochim. Acta 693 (2020), 178760.

[13] Y. Sutou, R. Kainuma, K. Ishida, Effect of alloying elements on the shape memory properties of ductile Cu–Al–Mn alloys, Mater. Sci. Eng., A 273 (1999) 375–379.

[14] Y. Sutou, et al., Development of medical guide wire of Cu-Al-Mn-base superelastic alloy with functionally graded characteristics, J. Biomed. Mater. Res. 69B (1) (Apr. 2004) 64–69, https://doi.org/10.1002/jbm.b.10079.

[15] Y. Araki, et al., Potential of superelastic Cu-Al-Mn alloy bars for seismic applications, Earthq. Eng. Struct. Dynam. 40 (1) (Jan. 2011) 107–115, https://doi.org/10.1002/eqe.1029.

[16] J.-L. Liu, H.-Y. Huang, J.-X. Xie, Superelastic anisotropy characteristics of columnar-grained Cu–Al–Mn shape memory alloys and its potential applications, Mater. Des. 85 (Nov. 2015) 211–220, https://doi.org/10.1016/j.matdes.2015.06.114.

[17] J. Van Humbeeck, Damping capacity of thermoelastic martensite in shape memory alloys, J. Alloys Compd. 355 (1–2) (Jun. 2003) 58–64, https://doi.org/10.1016/S0925-8388(03)00268-8.

[18] W. Elmay, et al., Damping capacity of Ti–Nb shape memory alloys evaluated through DMA and single-impact tests, Shape Mem. Superelasticity 8 (4) (Dec. 2022) 349–355, https://doi.org/10.1007/s40830-022-00398-7.